PNAS RESEARCH ARTICLE | MICROBIOLOGY

Proteo-genetic analysis reveals clear hierarchy of ESX-1 secretion in *Mycobacterium marinum*

Rachel M. Cronin[a], Micah J. Ferrell[a,1], Clare W. Cahir[a,2], Matthew M. Champion[b,3], and Patricia A. Champion[a,3]

Edited by Lalita Ramakrishnan, University of Cambridge, Cambridge, United Kingdom; received December 27, 2021; accepted May 6, 2022

The ESX-1 (ESAT-6-system-1) system and the protein substrates it transports are essential for mycobacterial pathogenesis. The precise ways that ESX-1 substrates contribute to virulence remains unknown. Several known ESX-1 substrates are also required for the secretion of other proteins. We used a proteo-genetic approach to construct high-resolution dependency relationships for the roles of individual ESX-1 substrates in secretion and virulence in *Mycobacterium marinum,* a pathogen of humans and animals. Characterizing a collection of *M. marinum* strains with in-frame deletions in each of the known ESX-1 substrate genes and the corresponding complementation strains, we demonstrate that ESX-1 substrates are differentially required for ESX-1 activity and for virulence. Using isobaric-tagged proteomics, we quantified the degree of requirement of each substrate on protein secretion. We conclusively defined distinct contributions of ESX-1 substrates in protein secretion. Our data reveal a hierarchy of ESX-1 substrate secretion, which supports a model for the composition of the extracytoplasmic ESX-1 secretory machinery. Overall, our proteo-genetic analysis demonstrates discrete roles for ESX-1 substrates in ESX-1 function and secretion in *M. marinum.*

ESX-1 | *Mycobacterium* | protein secretion | ESAT-6 | Type VII

Significance

ESX systems contribute to mycobacterial pathogenesis by transporting protein substrates into the host. The ESX-1 system is essential for bacterial survival in host immune cells. Several ESX-1 substrates are required for ESX-1–mediated protein transport, but the individual contributions to protein transport are unclear. We defined a hierarchy of ESX-1 secretion, which delineates a fundamental understanding of how ESX-1 substrates contribute to protein transport in *Mycobacterium marinum,* a model for *Mycobacterium tuberculosis* and other pathogenic mycobacterial species. We quantitatively defined the degree to which each ESX-1 substrate contributes to secretion of other proteins. The approach and the mechanistic insights into mycobacterial protein secretion may be generally applicable to other ESX-like systems in other species.

The bacterial pathogen, *Mycobacterium tuberculosis,* causes the human disease tuberculosis (1). Other pathogenic mycobacterial species cause disease in humans and in animals (2–4). *Mycobacterium marinum* is an occasional human pathogen that causes disease in ectothermic animals (5, 6). *M. tuberculosis* and *M. marinum* use conserved survival strategies during infection of host phagocytic cells (7, 8). Bacteria reside within and then damage the phagosome (9, 10), releasing the bacteria and their products into the cytoplasm (11, 12). Phagosomal damage triggers cytosolic host-response pathways. The released bacterial products dampen the host response to infection. The net result of phagosomal escape is host-cell lysis and bacterial spread (9, 11–13).

ESX-1 (ESAT-6 system 1) is a conserved protein secretion system that is essential for phagosomal damage (9, 14) and, consequently, mycobacterial virulence (15–17). Strains lacking an ESX-1 system are retained in the phagosome and attenuated (9, 14). The ESX-1 systems of *M. tuberculosis* and *M. marinum* are functionally interchangeable (18). *M. tuberculosis* ESX-1 substrate genes, regulatory genes, or Region of Difference-1 (RD1) genes complement mutations in the corresponding *M. marinum* genes (19–21), making *M. marinum* a popular model for studying the ESX-1 system (22).

The ESX-1 machinery includes six conserved proteins ($EccA_1$, $EccB_1$, $EccCa_1$, $EccCb_1$, $EccD_1$, $EccE_1$) that form a complex associated with the cytoplasmic membrane (23, 24). The machinery forms a pore that exports substrates, some of which are processed by the MycP1 protease (23, 25). ESX-1 substrates cross the mycobacterial outer membrane (MOM), localizing to the cell surface and the extracellular environment through an elusive mechanism (26). The majority of ESX-1 substrates are conserved between *M. tuberculosis* and *M. marinum* (6, 22), with additional *M. marinum*–specific substrates (27, 28). ESX-1 substrates include PE/PPE domain proteins of varying size; small, ∼100 amino acid WXG proteins; or glutamine- and alanine-rich proteins (22). PE/PPE proteins and WXG proteins from other ESX systems may contribute to transport across the mycolate outer membrane (29–31).

The functions of individual ESX-1 substrates are poorly defined. ESX-1 substrates may serve as regulators that control gene expression within the mycobacterial cell, as components of the secretory apparatus, or as effectors that disrupt membranes or function downstream of lysis (15, 21, 32–36). We have described multifunctional ESX-1 substrates that are regulators and effectors (21).

Substrates require each other for export (i.e., they are codependent), posing a major hurdle in understanding substrate function. Initial studies suggested that the deletion of any ESX-1 substrate gene resulted in attenuation in vivo and a complete loss of ESX-1–dependent protein secretion in vitro (16, 37). The number of ESX-1 substrates

Author contributions: M.M.C. and P.A.C. designed research; R.M.C., M.J.F., C.W.C., and M.M.C. performed research; R.M.C., M.J.F., and C.W.C. contributed new reagents/analytic tools; R.M.C., M.M.C., and P.A.C. analyzed data; and R.M.C., M.J.F., C.W.C., M.M.C., and P.A.C. wrote the paper.

The authors declare no competing interest.

This article is a PNAS Direct Submission.

[1]Present address: Department of Microbiology and Molecular Genetics, Michigan State University, East Lansing, MI 48824.

[2]Present address: Tri-Institutional Program in Chemical Biology, The Rockefeller University, New York, NY 10065.

[3]To whom correspondence may be addressed. Email: pchampio@nd.edu or mchampio@nd.edu.

This article contains supporting information online at http://www.pnas.org/lookup/suppl/doi:10.1073/pnas.2123100119/-/DCSupplemental.

Published June 7, 2022.

has since expanded (Fig. 1*A*) (19, 38–40). Several studies have used transposon-insertion mutagenesis or targeted approaches to disrupt substrate genes and define the role of ESX-1 substrates in secretion and host response (21, 27, 35, 39, 42–44). These approaches have often yielded contradictory results regarding the requirement of substrate genes. Recent studies in *M. marinum* and *M. tuberculosis*, including some from our laboratory, have demonstrated that codependent secretion can be uncoupled (21, 35, 38, 39, 43–47). However, a comprehensive quantitative measurement of the requirements of substrates for secretion is lacking.

We used a proteo-genetic approach (i.e., using genetics to inform the proteome) to define the specific contribution of each known ESX-1 substrate to protein secretion in *M. marinum* (48). We generated 12 *M. marinum* strains with unmarked deletions of individual ESX-1 substrate genes and the 12 corresponding complementation strains. We measured ESX-1 function in each *M. marinum* strain, demonstrating separable contributions by ESX-1 substrates to the lytic and cytolytic activity of *M. marinum*. Our studies identified *M. marinum* proteins with secretion profiles similar to ESX-1 substrates, and potential new ESX-1 substrates. We provide a model for the spatial order and transport of ESX-1 proteins across the MOM that is consistent with previous protein localization and interaction studies. Overall, our studies provide insight into the separable role of ESX-1 substrates in protein secretion and virulence.

Results

ESX-1 Substrates Are Differentially Required for Lytic Activity, Virulence, and Protein Secretion in *M. marinum*. We generated a collection of *M. marinum* M strains with unmarked deletions of each of the known ESX-1 substrate genes (Fig. 1*A* and *SI Appendix*, Table S1). We confirmed each strain using PCR (*SI Appendix*, Fig. S1) and targeted DNA sequencing. We generated complementation strains by introducing integrating plasmids expressing the substrate gene from the constitutive mycobacterial optimal promoter (49) or from endogenous promoters (*SI Appendix*, Table S1).

M. marinum lyses red blood cells in an ESX-1–dependent manner (42). Hemolytic activity may reflect ESX-1–dependent phagosomal damage during macrophage infection. If ESX-1 substrates were absolutely dependent on each other for function, we would expect hemolytic activity would be lost upon deletion of any substrate gene, similar to strains lacking the ESX-1 secretory machinery (e.g., Δ*eccCb$_1$*) (42). The expression of each substrate gene in the deletion strains would complement hemolytic activity to wild-type (WT) levels.

We measured the hemolytic activity of the 24 *M. marinum* deletion and complementation strains compared with the WT and Δ*eccCb$_1$* strains. Incubation of the sheep red blood cells with water controlled for maximal lysis. Incubation of sheep red blood cells with phosphate-buffered saline (PBS) was a cell-free control. The deletion of ESX-1 substrate genes revealed a continuum of hemolysis phenotypes (Fig. 1*B*, *SI Appendix*, Table S4). The Δ*eccCb$_1$* strain had significantly reduced hemolytic activity compared with the WT strain ($P < 0.0001$) (21, 27). Deletion of some substrate genes (*esxA, esxB, espB, espE, ppe68,* or *MMAR_2894*) resulted in hemolytic activity similar to the Δ*eccCb$_1$* strain and the cell-free (i.e., phosphate-buffered saline) controls. Strains lacking the *espA, espF, espJ,* or *espK* genes exhibited intermediate hemolytic activity that was significantly higher than the Δ*eccCb$_1$* strain ($P < 0.0001$) and significantly lower than the WT strain ($P < 0.0001$). The Δ*espF* strain exhibited intermediate hemolytic activity under the conditions tested. This activity was growth-phase dependent (*SI Appendix*, Fig. S2). Denser cultures of the Δ*espF* strain had hemolytic activity similar to the Δ*eccCb$_1$* strain (21). The Δ*espC* and Δ*pe35* strains exhibited WT hemolytic activity.

Complementation significantly increased hemolysis levels in all deletion strains with impaired hemolysis (Fig. 1*B*, compare *Right* with *Left*; $P < 0.0001$). In some strains, complementation restored hemolytic activity to near WT levels (Fig. 1*B*, Δ*esxB,* Δ*espA*, $P < 0.0001$; Δ*espC*, $P = 0.0047$; Δ*espJ*, $P = 0.0032$; Δ*espK*, $P = 0.0367$; Δ*ppe68*, $P = 0.0273$). From the complementation data, we conclude that deletion of specific ESX-1 substrate genes caused the observed changes in hemolytic activity. Together, these data demonstrate that ESX-1 substrates are differentially required for hemolysis.

The ESX-1 system is essential for mycobacterial pathogenesis (2, 12–15). Infection of phagocytic cells with *M. marinum* strains results in ESX-1–dependent host-cell lysis (9). We infected macrophage-like RAW 264.7 cells with the *M. marinum* strains at a multiplicity of infection of 5. We quantified cytolysis levels using ethidium homodimer-1 (EthD-1) staining at 24 h postinfection compared with the WT (virulent control) and Δ*eccCb$_1$* strains (attenuated control). EthD-1 is excluded from cells with intact cell membranes, but stains lysed cells with permeabilized membranes (50). Infection with WT *M. marinum* resulted in significantly higher levels of cytolysis than in the uninfected control ($P < 0.0001$; Fig. 1*C*).

Deletion of individual ESX-1 substrate genes resulted in a continuum of cytolytic activity (Fig. 1*C* and *SI Appendix*, Table S4). Infection with the Δ*esxA* and Δ*esxB* strains resulted in cytolysis levels similar to Δ*eccCb$_1$* infection. Expression of the *esxBA* operon restored macrophage lysis to WT levels. Infection with the Δ*espE* and Δ*espF* strains resulted in significantly reduced levels of cytolysis compared with the WT strain ($P < 0.0001$), as we previously reported (21). Like their hemolysis phenotypes, the Δ*espA,* Δ*espC*, and Δ*pe35* strains exhibited WT levels of cytolysis. Infection with these strains resulted in clumping of lysed macrophages and loss of the macrophage monolayer (*SI Appendix*, Fig. S3), which impacted detection and reduced EthD-1 cell counts. We suspect that the range of EthD-1–stained cells per field can be somewhat attributed to increased cytolytic activity of these strains compared with the WT strain.

Consistent with two prior reports (27, 51), the hemolytic and cytolytic activities did not strictly correlate. Some nonhemolytic strains were also noncytolytic (e.g., the Δ*esxA* and Δ*esxB* strains; compare Fig. 1 *B* and *C*). Other nonhemolytic strains retained significant levels of macrophage lysis (e.g., Δ*espB* and Δ*ppe68*), similar to the Δ*MMAR_2894* strain (27). In contrast, while the Δ*espK* strain was significantly more hemolytic than the Δ*eccCb$_1$* strain, the cytolytic activities of the Δ*espK* and Δ*eccCb$_1$* strains were similar.

Based on our hemolysis and cytolysis data, we hypothesized that individual ESX-1 substrates would differentially impact protein secretion. We generated cell-associated and secreted protein fractions from the 12 substrate deletion strains and the 12 complementation strains. We generated control protein fractions from the WT (ESX-1–secretion positive) and Δ*eccCb$_1$* (ESX-1–secretion negative) strains. Each set of substrate deletion strains was grown alongside matched WT and Δ*eccCb$_1$* strains to account for differences in growth and time.

EsxA and EsxB are highly secreted ESX-1 substrates in vitro. We measured production and secretion of EsxA and EsxB from each strain, using Western blot analysis (Fig. 1*D*). MPT-32

(a Sec-secreted protein) and the β subunit of RNA polymerase (a cell-associated protein) were loading and lysis controls, respectively. Each of the *M. marinum* strains, except the Δ*esxA* or Δ*esxB* strains, stably produced the EsxA and EsxB proteins (ESAT-6 and CFP-10; Fig. 1*D*, *Upper*, lanes 1–16). Deletion of the *esxA* or *esxB* genes resulted in the loss of both EsxA and EsxB (Fig. 1*D*, *Upper*, lanes 3 and 4) because they require each other for stability (16, 52). Differences in EsxA and EsxB levels produced in the substrate deletion strains were observed and can, in part, be explained by transcriptional regulation of the *esxBA* genes. For example, EsxA levels were reduced in the Δ*eccCb$_1$* strain (Fig. 1*D*, *Upper*, lanes 2 and 10) as compared with the WT strain (Fig. 1*D*, *Upper*, lanes 1 and 9), due to reduced *esxBA* transcription in the absence of the ESX-1 system (53). Likewise, EsxA and EsxB were elevated in the Δ*espE* strain (Fig. 1*D*, *Upper*, lane 8), due to increased *esxBA* gene expression in the absence of EspE or EspF (21).

The lower panels of Fig. 1*D* show the EsxA and EsxB secretion levels from each *M. marinum* strain (Fig. 1*D*, *Lower*, lanes 1–16). Some strains lacked detectable EsxA/EsxB secretion (Fig. 1*D*, *Lower*, lanes 15 and 16; Δ*ppe68* and Δ*MMAR_2894* strains), similar to the Δ*eccCb$_1$* strain, which lacks the secretory machinery (27). The remaining eight strains had reduced EsxA secretion compared with the WT strain, albeit to different levels. The majority of the ESX-1 substrate deletion strains did not substantially impact EsxB secretion. The Δ*espE* and Δ*espF* strains both showed intermediate EsxB secretion, as previously described (21).

Complementation restored production and secretion of EsxA and EsxB to near WT levels (Fig. 1*D*, lanes 19–24, 27–32). Expression of the *esxBA* operon in the Δ*esxA* and Δ*esxB* strains partially restored EsxA and EsxB production and secretion (lanes 19 and 20). These partial levels restored the cytolytic activity to WT levels for both strains, and restored the hemolytic activity for the Δ*esxA* complemented strain (Fig. 1 *B* and *C*). From these data we conclude that the ESX-1 substrate genes differentially contribute to the secretion of the EsxA and EsxB substrates. Overall, these data demonstrate that ESX-1 substrates have discrete and separable contributions to ESX-1–mediated hemolysis, host-cell cytolysis, and secretion.

Proteo-Genetic Analysis of *M. marinum* Secretion Reveals Distinct Secretory Profiles for ESX-1 Substrates. Our functional analysis of the ESX-1 substrate deletion collection revealed a continuum of phenotypes but did not yield clear results regarding separable roles of each substrate in ESX-1–associated functions. We partnered analytical measurement of the proteome with our genetic analyses to contextualize our observations regarding hemolysis and cytolysis.

We performed isobaric-tagging quantitative proteomics using iTRAQ to quantify changes to the *M. marinum* secretome in the 12 single-gene deletion strains and their complemented strains. Protein abundances were determined from at least two biological replicates and all were acquired in technical triplicate. A full repeated set of technical triplicates was performed on a separate liquid chromatography–mass spectrometry instrument to serve as quality control. Aggregate quantitative data are reported in Dataset S1, A. For the knockout strains (n = 18 individual samples × 8 iTRAQ reporters), 1,833 proteins and 18,433 peptides were identified at a 1% false discovery rate (54). The complement strain samples identified 1,475 proteins and 11,977 peptides at a 1% false discovery rate.

We visualized changes to *M. marinum* secretion by comparing the $\log_2$ fold change in protein levels secreted from each mutant and complemented strain with the levels secreted from the WT strain. This was achieved by reserving one of the eight iTRAQ channels (113 *m/z*) in each set of mutants for a culture-matched, WT-secreted proteome. As a result of this normalization to WT, all data can be compared as a common matched, fold-change ratio relative to the WT strain, enabling global ratio comparisons to be accurate even from ratios originating in different experiments.

We visualized these relationships using a clustered heat map to observe similarities between overall secreted proteomes for each strain (*x*-axis) and similarities in the secreted levels for each measured protein (*y*-axis; Fig. 2*A*). The levels of the majority of the secreted proteins measured were unchanged by deletion or expression of ESX-1 substrate genes as compared with those secreted from the WT strain (yellow). Measured changes in protein secretion from each mutant strain were generally restored by complementation, since the majority of the complemented strains clustered in the heat map. The Δ*esxB/pesxBA* strain did not cluster with the other complementation strains, likely reflecting the incomplete complementation observed in Fig. 1 *B* and *D*. A readable version of the heat map is in *SI Appendix*, Fig. S4.

The known ESX-1 substrates that we confidently detected were clustered into several distinct clades within the heat map, indicating shared requirements for secretion (Fig. 2*B*). Several substrates clustered with established partners. EsxA and EsxB clustered together. EsxA and EsxB directly interact and are secreted as a substrate pair (16, 52). EspA and EspC interact with each other (32) and were clustered in a clade. EspB and EspK directly interact (19) and were clustered in a clade with EspJ. EspE and EspF clustered together and require each other for secretion (21). We were unable to quantify MMAR_2894 reliably in this study, likely because of isobaric interference. We were also unable to detect PE35. Overall, the four distinct ESX-1 clades demonstrate that ESX-1 substrates have at least four distinct secretory profiles. These data support that the requirement of the ESX-1 substrates for proteins secretion is not equivalent.

We identified several clades that significantly correlated with the ESX-1 substrates, using Pearson correlation (Fig. 2*C*, data are provided in Dataset S1, C, and *P* values are reported in Dataset S1, D). Proteins that significantly clustered with ESX-1 substrates are secreted proteins or present in the mycobacterial cell membrane fractions but have not been associated with ESX-1 (41, 55–59). Secretion of MPT-64, a protein secreted independently of ESX-1, did not significantly correlate with the ESX-1 substrates. Although secretion of MPT-64 significantly correlated with four of the proteins, the correlation was weaker than the correlation with ESX-1 secretion. The specific proteins are discussed in the *SI Appendix*. These data indicate that the secretion of several additional proteins significantly correlate with the secretion of known ESX-1 substrates.

Establishing the Core, Secreted ESX-1–Dependent Proteins from *M. marinum*. EccCb$_1$ is an essential component of the secretory apparatus (16). The EsxA and EsxB substrates are required for the secretion of the known ESX-1 substrates and are likely components of the secretory apparatus (22). We reasoned that analyzing which proteins exhibited reduced secretion upon the loss of EccCb$_1$, EsxA, and EsxB may reveal a core set of ESX-1–secreted proteins.

We compared the $\log_2$ fold change of the level of each protein in the secreted fractions from the Δ*eccCb$_1$*, Δ*esxA*, or Δ*esxB* strains normalized to the WT strain (mutant/WT) with

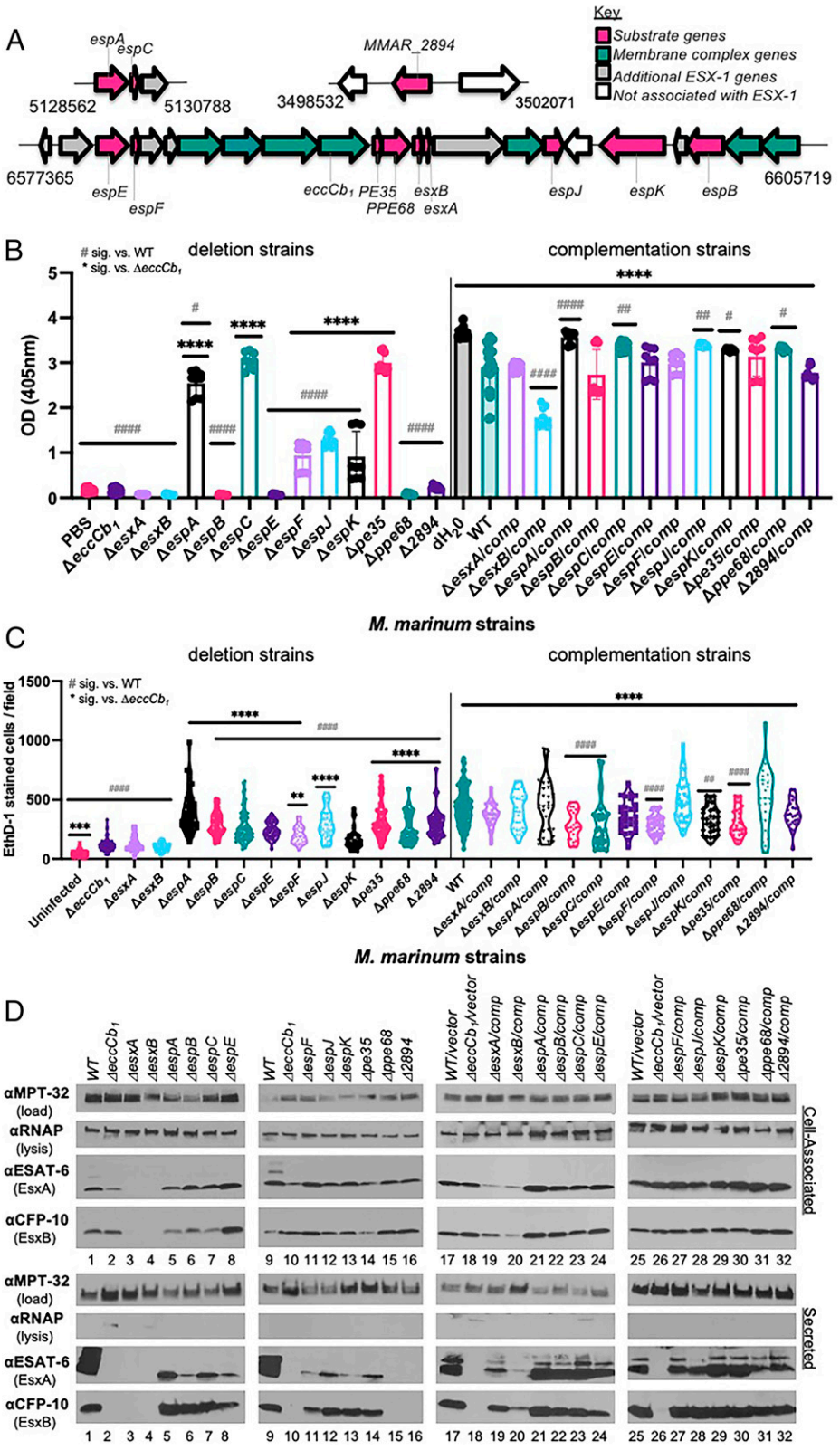

Fig. 1. ESX-1 substrates are differentially required for EsxA/B secretion and function. (*A*) The ESX-1 locus and accessory loci. Substrate genes are in pink. The conserved secretory component genes are in teal, including the *eccCb*$_1$ gene. Numbers represent *M. marinum* genome position from Mycobrowser (54). Strains are listed in *SI Appendix*, Table S1. (*B*) Hemolytic activity of ESX-1 substrate deletion strains (*Left*) and complementation strains (*Right*). Data are the average of at least three biological replicates, in technical triplicate. Dots indicate technical replicates, bars indicate the mean. Error bars are the SD. Statistical significance (sig.) was determined using a one-way ordinary ANOVA ($P < 0.001$) followed by a Tukey's multiple comparison test. The hemolytic activity of the Δ*eccCb*$_1$ strain was not different from that of the cell-free control (PBS). Significance compared with the Δ*eccCb*$_1$ (*), compared with the WT strain ($^{\#}$). $^{\#}$Δ*espK/comp,* $P = 0.0112$; $^{\#}$Δ*espA,* $P = 0.0247$; $^{\#}$Δ*ppe68/comp,* $P = 0.0273$; $^{\#\#}P = 0.0066$, $^{\#\#\#}$Δ*espC/comp,* $P = 0.0047$; $^{\#\#\#\#}$Δ*espJ*/comp, $P = 0.0032$; $^{\#\#\#\#}$ and $^{****}P < 0.0001$. (*C*) Macrophage infection of ESX-1 substrate deletion strains (*Left*) and complementation strains (*Right*). Data are the average of at least three biological replicates, each in technical triplicate. EthD-1–stained cells were counted from five fields from each well, represented by dots. Statistical significance was determined using a one-way ordinary ANOVA ($P < 0.0001$) followed by a Tukey's multiple comparison test. Significance compared to the Δ*eccCb*$_1$ (*), compared to the WT strain ($^{\#}$). The cytolytic activity of the Δ*eccCb*$_1$ strain was significantly different from that of the cell-free control ($^{***}P = 0.0009$). **** or $^{\#\#\#\#}P < 0.0001$, $^{**}P = 0.0053$, $^{\#\#}P = 0.0043$. A summary of hemolytic and cytolytic activity is given in *SI Appendix*, Table S4. (*D*) Western blot analysis measuring protein secretion. Protein (10 μg) was loaded in each lane. Western blots are representative of at least three biological replicates. OD, optical density.

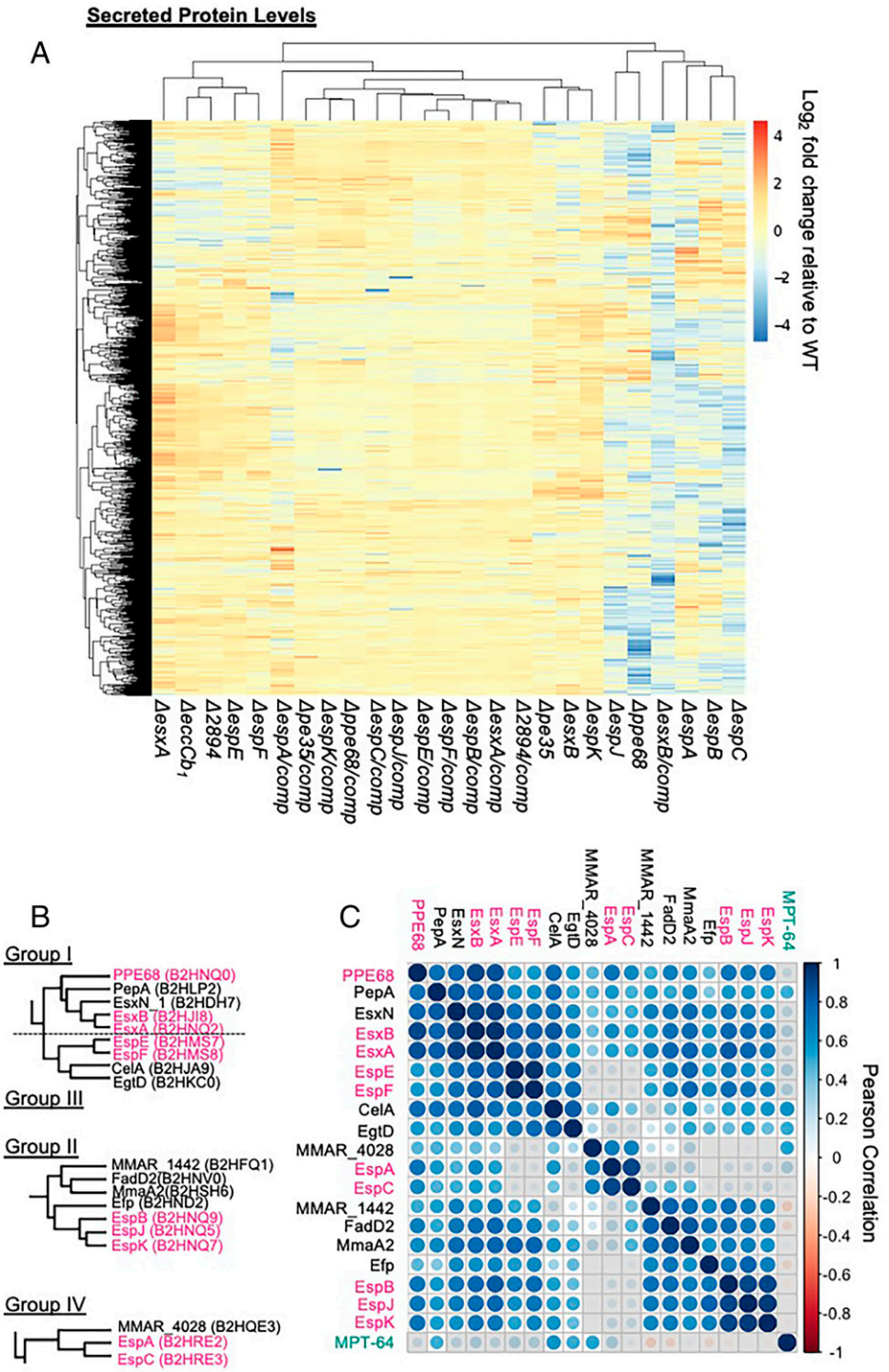

Fig. 2. Impact of ESX-1 genes on the *M. marinum* proteome. (*A*) Heat map of the *M. marinum* proteome. Values are the $\log_2$ fold change of each protein (*y*-axis) in the strains indicated (*x*-axis) compared with the detected levels from the WT strain. Proteins secreted from the mutant strains but not the WT strain or vice versa were excluded. Data are reported in Dataset S1, B. (*B*) Clustering of known ESX-1 substrates with additional *M. marinum* proteins. These clusters were taken from the readable heat map in *SI Appendix*, Fig. S4. Dotted line denotes separation of groups I and III. (*C*) Pearson correlation of protein secretion (calculated from $\log_2$ fold change from all mutant and complemented strains compared with the WT strain). Known ESX-1 substrates are labeled in pink; additional proteins are from *B*. Gray boxes indicate that the correlation is not statistically significant. The size of the circle corresponds to significance. The data are reported in Dataset S1, C. The *P* values for the Pearson correlation are reported in Dataset S1, D.

the significance ($\log_{10}$ *P* value). We focused on proteins with reduced secretion, but there were proteins with increased secretion from these mutant strains. Deletion of the *eccCb*$_1$, *esxA*, or *esxB* genes resulted in significant changes to the secretion of a low number of proteins (Fig. 3*A*, *SI Appendix*, Fig. S5 and data in Dataset S2). To define rigorous parameters to measure substrate dependency, we first used a cutoff of $\log_2$ fold change of ≥ 1, with $P < 0.05$. Using these parameters, the secretion of 9, 17, and 10 proteins was significantly reduced from the Δ*eccCb*$_1$, Δ*esxA*, and Δ*esxB M. marinum* strains as compared with the WT strain ($\log_2$ fold change ≥ 1; $P < 0.05$). The secretion of a majority of these proteins was restored upon expression of the *esxBA* operon in the Δ*esxA* (Fig. 3*A*, *Right*) or Δ*esxB* strains (*SI Appendix*, Fig. S5).

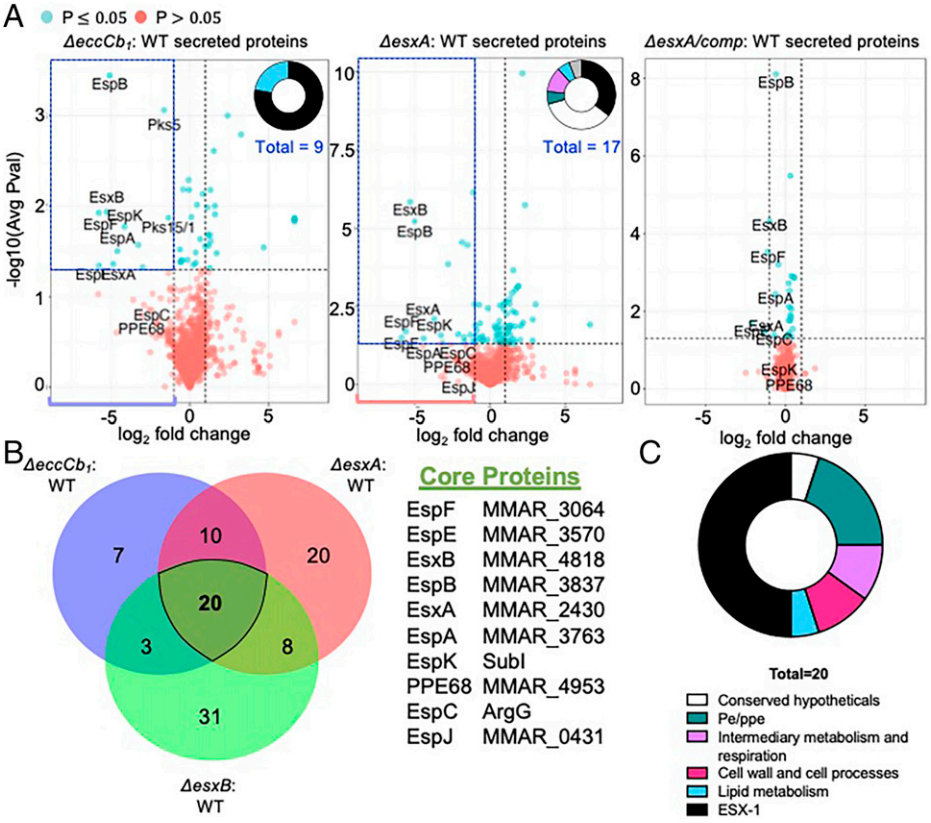

Fig. 3. Core *M. marinum* proteins dependent on ESX-1 for secretion. (*A*) Volcano plots of proteins measured in the Δ*eccCb*$_1$, Δ*esxA*, and Δ*esxA* complemented strains. The $\log_2$ fold change of secretion from each strain normalized to the WT strain is plotted against $\log_{10}$ of the *P* value. Horizontal black dashed line signifies $P = 0.05$; blue dots indicate $P \leq 0.05$; red dots indicate $P > 0.05$. Vertical, black dashed lines signify a $\log_2$ fold change = 1, 1. ESX-1 substrates are labeled. The donut plots are functional analyses of *M. marinum* proteins in the quadrant indicated by the blue dashed lines. The purple and red brackets at the bottom left of the volcano plots signify the proteins used in *B*. The data are reported in Dataset S2. (*B*) Venn diagram of the proteins with reduced secretion in the Δ*eccCb*$_1$, Δ*esxA*, and Δ*esxB* strains (*SI Appendix*, Fig. S5) as compared with the WT strains. (*C*) Functional analysis of the 20 core proteins identified in *B*. All functional classifications were obtained from Mycobrowser. Avg, average; Pval, *P* value.

The secretion of the ESX-1 substrates was significantly reduced from all three strains compared with the WT strain. The secretion of seven ESX-1 substrates was significantly reduced from the Δ*eccCb*$_1$ strain (EsxA, EsxB, EspA, EspB, EspE, EspF, EspK, labeled in Fig. 3*A*, black slice donut plot; Dataset S2). The secretion of six (EsxA, EsxB, EspB, EspE, EspF, and EspK) and four (EsxB, EspB, EspF and EspK) ESX-1 proteins was reduced from the Δ*esxA* and Δ*esxB* strains, respectively. Two additional proteins with significantly decreased secretion from the Δ*eccCb*$_1$ strain were involved in lipid metabolism (Pks5, Pks15/1). Both proteins are membrane-localized polyketide synthases in *M. tuberculosis*, making them probable membrane proteins in *M. marinum* (41, 55, 58). A small number of additional proteins, including PE/PPE proteins (also secreted by ESX systems), lipid metabolism and intermediary metabolism proteins, conserved hypotheticals, and proteins of unknown function had significantly reduced secretion from the Δ*esxA* or Δ*esxB* strains compared with the WT strain ($n = 11$ and 6 proteins, respectively).

Several ESX-1 substrates had reduced secretion from these strains but did not meet our *P* value threshold ($P < 0.05$). We hypothesized that this was due to low or no expression of some proteins in some of the mutant strains. EspC, EspJ, and PPE68 secretion was reduced in the Δ*eccCb*$_1$ strain relative to the WT strain, but the significance of this change did not meet our *P* value threshold. EspJ, in particular, has poor proteotypic properties, producing only a single tryptic peptide with high reliability. However, we did detect each protein in the complemented strains. We previously demonstrated that strict significance cutoffs in quantifying components that are genetically absent underrepresents phenotypic changes because significance cutoffs are less reliable with missing values in strains (53, 60). Because known ESX-1 substrates fell below the *P* value cutoff, we compared the proteins whose secretion was reduced by a $\log_2$ fold change ≥1 in the Δ*eccCb*$_1$, Δ*esxA*, and Δ*esxB* strains (Fig. 3*B*, brackets in Fig. 3*A* and *SI Appendix*, Fig. S5) with the WT strain. We identified 20 proteins with reduced secretion in all three strains relative to the WT strain (Fig. 3*B*). These 20 proteins included all 10 known ESX-1 substrates that we could reliably measure, consistent with a loss of ESX-1 secretion in these strains.

The 10 proteins not previously associated with the ESX-1 system (Fig. 3*B*) included PE/PGRS proteins, proteins involved in cell-wall processes, and proteins involved in metabolism (Fig. 3*C*) (41). For 8 of the 10 proteins, bioinformatic analysis of predicted signal sequences (61) were predicted as "other" (i.e., neither predicted Sec nor Tat substrates), similar to the known ESX-1 substrates. Four of the 10 proteins were predicted PE/PGRS, and one had a predicted WXG motif. All five had predicted helices at the protein N termini, similar to known ESX-1 substrates (*SI Appendix*, Fig. S6). We conclude that we have established a core set of ESX-1–dependent proteins, which includes additional proteins in *M. marinum* that may be potential ESX-1 substrates.

ESX-1 Substrates Are Differentially Required for Substrate Secretion. To conclusively define the extent of substrate dependency, we analyzed secretion from the substrate deletion strains. The quantitative differences in each proteome represent differences

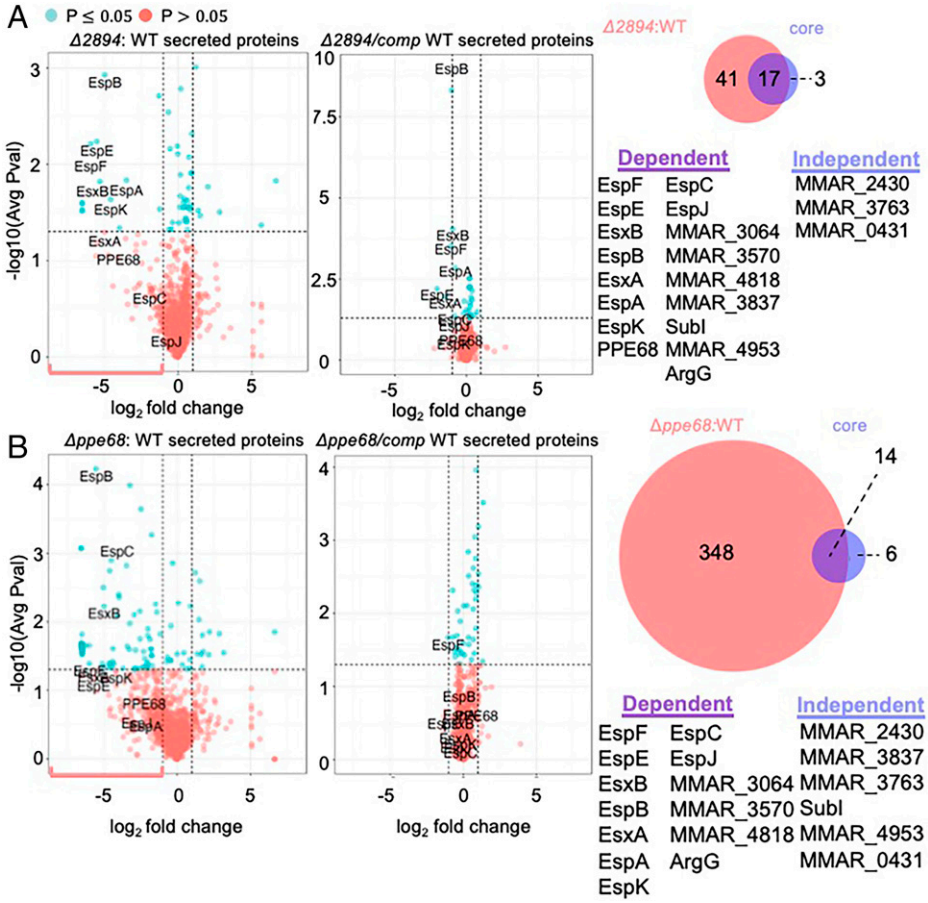

Fig. 4. Group I substrates PPE68 and MMAR_2894 (PE) are required for the secretion of all known ESX-1 substrates. Volcano plots of protein levels of proteins in the secreted fractions from *A*. The Δ*MMAR_2894* strain or the Δ*MMAR_2894* complemented strains or (*B*) Δ*ppe68* or Δ*ppe68* complemented strains compared with the WT strain. The blue box represents the cutoff of $\log_2$ fold change ≥ to 1 and $P < 0.05$. The red bracket indicates those proteins with a $\log_2$ fold change ≥1, regardless of *P* value. These proteins were used in the Venn diagrams (right) compared with the core proteins identified in Fig. 3. Avg, average; Pval, *P* value.

in secretion that are dependent upon the loss of each individual substrate. We grouped the substrates into four groups based on the clustering shown in Fig. 2 and how the loss of each substrate impacted the secretion of the other ESX-1 substrates.

The deletion (Fig. 4 *A* and *B*, *Left*) of the *ppe68* or *MMAR_2894* genes resulted in changes to the *M. marinum* secretome, including the known ESX-1 substrates (labeled in Fig. 4 *A* and *B*). Complementation of each gene (Fig. 4 *A* and *B*, *Right*) restored protein secretion to near WT levels. Based on our analyses of the Δ*eccCb*$_1$, Δ*esxA*, and Δ*esxB* strains, we considered the proteins impacted by the loss of the *MMAR_2894* and *ppe68* genes by a $\log_2$ fold change ≥1 (pink brackets Fig. 4 *A* and *B*; compare with Fig. 3). We compared these proteins ($n = 58$ from the Δ*MMAR_2894* strain; $n = 362$ from the Δ*ppe68* strain, respectively) with the 20 "core proteins" (Venn diagrams in Fig. 4). PPE68 and MMAR_2894 were required, to varying extents, for the WT secretion of all of the known ESX-1 substrates. PPE68 and MMAR_2894 were also required for WT levels of secretion several additional core proteins (Dataset S2). Consistent with these findings, both PPE68 and MMAR_2894 were required for hemolysis and were partially cytolytic (Fig. 1). From these data, we propose that PPE68 and MMAR_2894 are secreted components of the ESX-1 secretory apparatus, similar to EsxA and EsxB. In the remainder of this article, we refer to EsxA, EsxB, PPE68, and MMAR_2894 as group I substrates.

Deletion of the *ppe68* and *MMAR_2894* genes resulted in changes to additional proteins outside of the core (Dataset S2). Based on the overall changes to the mycobacterial proteome in the absence of PPE68 and MMAR_2894, we conclude that these proteins may have distinct roles in mycobacterial physiology beyond roles in ESX-1 substrate secretion.

We performed the same analyses on the remaining strains lacking individual ESX-1 substrate genes. We grouped the remaining substrates into three additional groups based upon how they clustered in Fig. 2*B*, and we analyzed how they impacted the secretion of the known ESX-1 substrates, using a $\log_2$ fold change cutoff of ≥1 relative to the WT strain. We placed EspB, EspJ, and EspK into group II, EspE and EspF into group III, and EspA and EspC into group IV, as defined below. Individual quantitative plots and Venn diagrams are in *SI Appendix*, Figs. S7–S9.

The substrates in group II clustered together, as shown in Fig. 2*B*. The loss of EspB, EspK, and EspJ resulted in a reduction ($\log_2$ fold change ≥1 relative to the WT strain) of the secretion of group III, but not group IV substrates (*SI Appendix*, Fig. S7). Group III substrates clustered together, as shown in Fig. 2*B*. The loss of either EspE or EspF did not impact the secretion of group II or group IV substrates (*SI Appendix*, Fig. S8). The requirements for group IV substrates, which also clustered together, were less clear from these analyses, but it appeared that EspC was only required for EspA secretion (*SI Appendix*, Fig. S9).

Loss of substrates in these groups had differing effects on the overall proteome. For example, EspK (group II) and EspE and

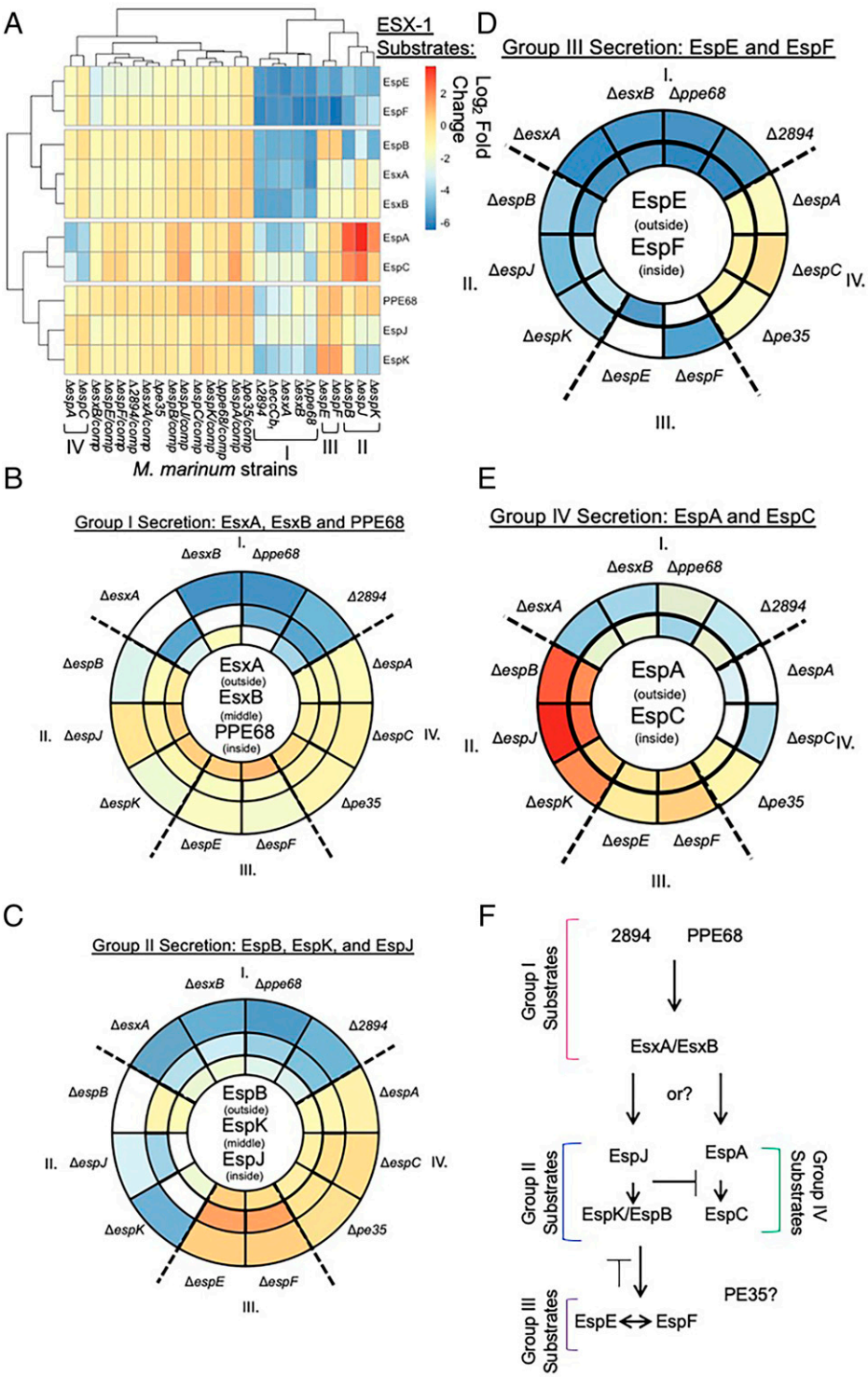

Fig. 5. ESX-1 substrates are differentially required for ESX-1–dependent secretion. (*A*) Heat map of the $\log_2$ fold change (mutant/WT levels) of ESX-1 substrate levels in *M. marinum* strains lacking specific ESX-1 substrate genes and their complementation strains. The data are reported in Dataset S1, E. Visualizations of the relative impact of each substrate deletion on (*B*) group I (*C*) group II or (*D*) group III or (*E*) group IV substrates. Substrates of interest are shown in the circles. Sector colors match the levels in the heat map in *A*. I, II, III, and IV refer to the substrate groups, which are separated by a dotted line. The deletion strains for each substrate are white sectors. (*F*) Proposed order of substrate secretion. Avg, average; Pval, *P* value.

EspF (group III) substrates impacted few proteins outside of the core proteins. In contrast, EspB and EspJ (group II) and the group IV substrates impacted the proteome more broadly. Together, these data demonstrate that the ESX-1 substrates differentially contribute to ESX-1 secretion and may have unique, broader impacts on the levels of proteins secreted into the culture media, either directly or indirectly.

Defining the Relationships between ESX-1 Substrates Reveals Relative Levels of Substrate Dependency. To define the relationships between ESX-1 substrate groups, we generated a heat map of the $\log_2$ fold change (mutant/WT levels) of ESX-1 substrate levels secreted from *M. marinum* strains lacking specific ESX-1 substrate genes and their isogenic complementation strains (Fig. 5*A* and Dataset S1, E and F, for relative changes in

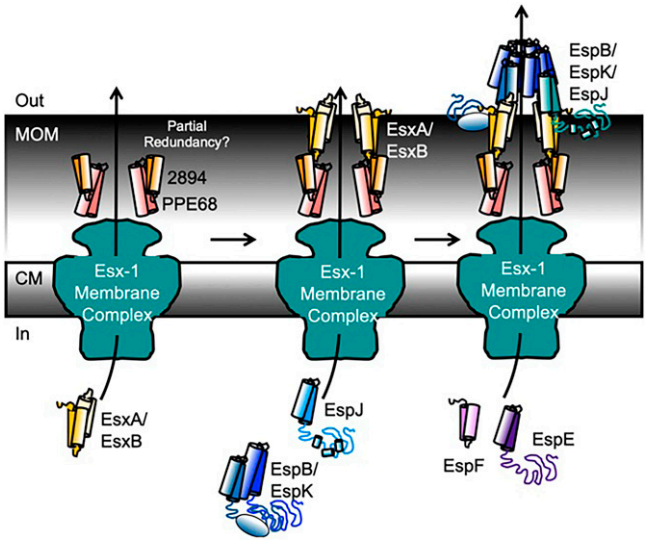

Fig. 6. Model for hierarchical secretion of ESX-1 substrates and secretory apparatus. We propose an inside-out assembly mechanism, whereby several ESX-1 substrates are hierarchically secreted to form structural components of the ESX-1 secretory machinery. CM, cytoplasmic membrane.

ESX-1 substrates). The Δ*eccCb*$_1$ strain exhibited reduced secretion of all known ESX-1 substrates, as indicated by the blue and green colors on the heat map (Fig. 5*A*). The additional strains clustered into the groups similar to those we identified by analyzing the volcano plots (Fig. 5*A*). *M. marinum* strains lacking the group I substrates, Δ*esxA,* Δ*esxB,* Δ*ppe68*, and Δ*MMAR_2894*, all clustered with the Δ*eccCb*$_1$ *M. marinum* strain, consistent with these substrates being part of the secretory apparatus.

To interpret the heat map, we visualized the relationships between substrates (Fig. 5 *B–E*). The sectors are colored based on the $\log_2$ fold change in the heat map (Fig. 5*A*) to visualize the magnitude of the dependence between the substrates for secretion. Comparing the relative requirements of each substrate gene for the secretion of each substrate (Fig. 5 *B–E*, circled in middle) revealed patterns demonstrating that the requirement between ESX-1 substrates is not equivalent. The secretion of the group I substrates (EsxA, EsxB, and PPE68) was most impacted by other group I substrates (EsxA, EsxB, PPE68, and MMAR_2894), as indicated by the dark blue sectors (Fig. 5*B*). In contrast, the contributions of the substrates in groups II, III, and IV to the secretion of group I substrates was minimal (yellow sectors, $\log_2$ fold change numbers in Dataset S1, E).

Although group I substrates were dependent upon each other, a hierarchy of dependency was established. MMAR_2894 greatly impacted the secretion of EsxA, EsxB, and PPE68. Although we did not consistently detect MMAR_2894, we tested the requirement of PPE68, EsxA, and EsxB for MMAR_2894 secretion (*SI Appendix*, Fig. S10). We constitutively expressed *MMAR_2894* with a C-terminal Strep-tag (27) in the Δ*ppe68,* Δ*esxA*, and Δ*esxB* strains and measured secretion of MMAR_2894-ST compared with the WT and Δ*eccCb*$_1$ strains. While PPE68 was required for MMAR_2894-ST secretion (*SI Appendix*, Fig. S10*A*), EsxA and EsxB were dispensable (*SI Appendix*, Fig. S10*B*). Constitutive expression of MMAR_2894-ST in the Δ*ppe68* strain did not restore EsxB secretion (*SI Appendix*, Fig. S10*A*).

Because PPE68 and MMAR_2894 require each other for secretion and are required for the secretion of all of the additional substrates, we were surprised that deletion of either *ppe68* or *MMAR_2894* was insufficient to block cytolysis (Fig. 1*C*). To understand the relationship between PPE68 and MMAR_2894, we generated a Δ*ppe68* Δ*MMAR_2894* strain. The resulting double-deletion strain was nonhemolytic and exhibited cytolytic activity similar to the Δ*eccCb*$_1$ strain (*SI Appendix*, Fig. S10 *C–E*). Together these data indicate that MMAR_2894 and PPE68 are partially redundant for ESX-1 secretion, consistent with the divergent changes caused by the loss of either to the *M. marinum* secretome (Fig. 4)

PPE68 greatly impacted the secretion of EsxA and EsxB. Although EsxA and EsxB required each other for secretion, EsxA and EsxB had a lesser impact on PPE68 secretion than MMAR_2894 did on PPE68 secretion. From these data, we propose that PPE68 and MMAR_2894 are secreted prior to and are required for the secretion of EsxA/EsxB (Fig. 5*F*). We also observed this requirement by Western blot analysis (Fig. 1*D*).

The loss of any of the four group I substrates specifically and negatively impacted the secretion of the group II substrates, EspB, EspJ, and EspK (Fig. 5*C*). The greatest dependencies in group II were the requirement of EspJ for EspK secretion and the requirement of EspK for EspB secretion, as reported (19). Any requirement of EspA, EspC, or PE35 on the secretion of the group II substrates was less than that of the group I substrates (yellow sectors). The loss of the group III (EspE or EspF) substrates resulted in increased secretion of EspK, EspB, and EspJ (Fig. 5*C*, orange sectors). From these data, we propose that the group II substrates require group I substrates for protein secretion but not group III or group IV substrates. Therefore, we propose that group II substrates are secreted after group I substrates, and that EspJ is secreted prior to EspB and EspK (Fig. 5*F*).

The loss of any of the group I or group II substrates negatively impacted the secretion of EspE and EspF (Fig. 5*D*, blue sectors). The requirement for group I substrates was stronger than for the group II substrates (Fig. 5*D*, darker blue sectors). group IV substrates had relatively little impact on the secretion of EspE and EspF (Fig. 5*D*, yellow sectors). Notably, as previously demonstrated, EspE and EspF were each required for the other's secretion (21). From these data, we propose that group III substrates require group I and group II substrates but not group IV substrates for secretion.

Finally, the group I substrates were most required for the secretion of the EspA and EspC group IV substrates (Fig. 5*E*, blue and green sectors). In particular EsxA, EsxB, and MMAR_2894 were the substrates most required for EspA, while PPE68 was most important for EspC (Fig. 5*E*). EspA and EspC require each other for secretion (32). Interestingly, the loss of group II substrates and, to a lesser extent, group III substrates resulted in increased secretion of both EspA and EspC (Fig. 5*E*, orange and red sectors). From these data, we propose that EspA and EspC substrates are either regulated by or compete for secretion with group II and group III substrates (Fig. 5*F*). Overall, these data order protein secretion by ESX-1, demonstrating that the dependency of secretion among ESX-1 substrates is not equivalent and allowing inference into function.

Discussion

We provide a comprehensive proteo-genetic analysis of the contribution of the known ESX-1 substrate genes to protein secretion in *M. marinum.* Our genetic analyses showed that ESX-1 substrates are differentially required for hemolytic activity and macrophage cytolysis. Our quantitative analyses revealed at least four groups of ESX-1 substrates that differentially impacted protein secretion. We identified proteins that significantly

correlate with ESX-1 substrate secretion or that may be potential ESX-1 substrates. Finally, our proteo-genetic analysis implies a proposed order of hierarchical protein secretion and transport, which is poised to be tested further in *M. marinum, M. tuberculosis*, and in other mycobacterial species with ESX-1 systems.

Our data support a testable model for the role of ESX-1 substrates in protein secretion, which we place in the context of findings from the field (Fig. 6). We propose that the sequential secretion of ESX-1 substrates implies an "inside-out" assembly, similar to alternative secretory and flagellar machines in which the extracytoplasmic subunits are transported through the exporter in the cytoplasmic membrane (62). Several ESX-1 substrates are likely structural components of the transport machinery that span the MOM and traverse the surface of the mycobacterial cell.

We suggest that the group I substrates form the channel connecting the Ecc conserved components in the membrane with the mycobacterial cell surface. We showed that PPE68 and MMAR_2894 require each other for secretion and are required for the secretion of all other substrates, including EsxA and EsxB. We propose that PPE68 and MMAR_2894 physically form part of the channel in the periplasm and across the MOM. PPE68 has been localized to the mycobacterial cell envelope (63). Prior studies support that PE/PPE proteins are transporters in the MOM (30, 31, 64, 65) and may transport ESX proteins (66). The use of PE/PPE proteins to transport across the MOM could be dynamic, allowing for the use of multiple PE/PPE proteins under different conditions. The deletion of the *MMAR_2894* or *ppe68* genes resulted in reduced cytotoxicity (Fig. 1 and ref. 27), suggesting that the two proteins have some degree of functional redundancy. Because *MMAR_2894* is not conserved in *M. tuberculosis,* additional PE proteins may substitute for MMAR_2894. Although not yet a general phenomenon, specific PE/PPE pairs have been shown to switch partners, forming functional pairs with additional noncognate PE/PPE proteins (30).

EsxA and EsxB potentially make up the remaining part of the transporter that crosses the surface of the MOM. Our data show that while PPE68 and MMAR_2894 have a large impact on EsxA/EsxB secretion, the reverse is not true. EsxA/EsxB are required for the secretion of the remaining substrates. EsxA and EsxB directly interact (16, 67) and are surface localized and detected in the culture supernatant during growth in vitro (15, 16, 42, 50, 59, 68). Esx proteins paralogous to EsxA and EsxB are required for protein secretion across the MOM (64). Finally, a direct interaction between EsxA and PPE68 has been reported, connecting the two parts of the proposed trans-MOM machinery (Fig. 6) (64).

ESX-1 substrates have been proposed to form rings (EspB) or filaments (EspC) that form either a channel or a "needle" (32–34). Neither of these proteins is required for WT levels of ESX-1 substrate secretion, which may be explained by our model. We propose that following the secretion of the group I substrates, the group II substrates, EspB/EspK and EspJ, are secreted. The contribution of these three proteins to group I substrate secretion is relatively minimal, placing them next in the secretory order (Fig. 5). These three proteins may extend the ESX-1 secretory apparatus from the mycobacterial cell surface (Fig. 6).

Our data show that EspJ is required for EspB and EspK secretion. EspB and EspK directly interact (19). EspJ interacts with the EsxB when partnered with EsxA (69), providing a direct connection between the EsxB/A proteins and this part of the secretory apparatus. During secretion, EspB is processed by the MycP1 protease, an essential part of the ESX-1 secretory apparatus (24, 70). The processed form of EspB, which corresponds to its N-terminal half, forms heptameric rings (33). EspK functions to keep EspB from oligomerizing inside of the mycobacterial cell (71).

EspE and EspF (group III) are likely secreted following group II. Our data show that group I and group II substrates are required for EspE and EspF secretion (Fig. 5). EspE and EspF negatively regulate ESX-1 substrate gene expression (21). This relationship is reflected in Fig. 5 *B* and *C* (orange sectors); deletion of the *espE* or *espF* genes increased the secretion of group I and group II substrates as compared with the WT strain. Similar increases in substrate secretion following the loss of substrates with regulatory roles have been reported in type III secretion systems (62, 72, 73).

EspE and EspF are required for hemolytic activity and for macrophage lysis (Fig. 1 *SI Appendix*, Fig. S2, and ref. 21). EsxA and EsxB may be required for lytic activity because they are required for EspE and EspF secretion. The reverse is not possible, because EspE and EspF are not required for the secretion of EsxA and EsxB. Alternatively, several ESX-1 substrates, including EspE and EspF, may form a multipartite cytolytic toxin, similar to MakABE in *Vibrio cholerae* (74).

EspA and EspC (group IV) are essential for ESX-1 secretion and virulence in *M. tuberculosis* (37, 75, 76). Our data show that EspA and EspC are relatively dispensable for the secretion of ESX-1 substrates, for hemolytic activity, and for macrophage lysis in *M. marinum*. In contrast, the *espA* and *espC* genes are paralogous to the *espE* and *espF* genes (37, 38, 75). The role or regulation of these substrates may diverge between *M. marinum* and *M. tuberculosis.* However, our data were insufficiently resolved to incorporate this group of substrates into the ordered assembly. Different infection models or in vitro growth conditions could allow incorporation of these proteins into the model.

Deletion of group II substrates increased EspA and EspC secretion. Based on the type III secretion literature, several possible relationships may explain our data. First, the group II substrates may regulate the expression of the *espACD* operon. Alternatively, the group II substrates could broadly regulate secretion, similar to PcrV in *Pseudomonas* (77). Deletion of the *pcrV* gene results in constitutive unregulated secretion (77). Second, based upon type III secretion in *Yersinia,* the group II substrates may function as molecular rulers that regulate the length of the secretory apparatus. Deletion of the YscP ruler in *Yersinia* results in increased substrate secretion (78). Finally, the group II substrates may be higher-affinity substrates for secretion than the group IV substrates. In the absence of the group II substrates, there may be less competition for secretion, resulting in hypersecretion of the group IV substrates. These mechanisms need to be tested at the molecular level.

A major strength of our study is the scale and the use of unmarked deletions and genetic complementation, which, together, allowed us to identify changes in secretion caused specifically by the loss of individual substrate genes. Prior studies revealed uncoupling of ESX-1 substrate dependency by focusing on the interactions between a small number of substrates (27, 43, 44, 46) or by using transposon-insertion strains to define the dependency between substrate secretion (39, 42) or host phenotypes (35, 47). Our study builds on these findings and confirms, solidifies, and expands our understanding of the specific ordered contributions of ESX-1 substrates to secretion. Importantly, our studies revealed and resolved inconsistencies

in the literature regarding the requirement of EspB, EspK, EspJ, and EspE in the secretion of EsxA and EsxB (*SI Appendix*, Table S5) as compared with studies using transposon-insertion strains (35, 39, 42). Because EspA and EspC are dispensable for ESX-1 secretion in *M. marinum*, it is difficult to compare some of our findings with studies of *M. tuberculosis* (43, 44, 47, 79). We previously (27) measured secretion from the Δ*MMAR_2894* strain using an independent proteomics approach (Label Free Quant). We can directly compare the fold-changes in secretion between our present and prior study for the role of MMAR_2894 in secretion. Both studies consistently reported decreased secretion of eight known substrates in the same direction and magnitude. The relative levels of EspF, EspB, and EspA secretion from the *MMAR_2894* differ by less than a $\log_2$ of 1; EspE, EsxB, EspK, and PPE68 by $\log_2 \cong 3$; and EspJ by $\log_2$ of 7.7. EspJ was not well measured in the previous study and is problematic for proteomics, as described earlier.

This study has yielded the largest quantitative dataset of ESX-1 protein secretion to date, to our knowledge. We focused on the secretome to glean insight into how each ESX-1 substrate contributes to protein secretion. A caveat is that while the substrate dependencies imply a hierarchy of secretion, the complex interactions between substrates in the mycobacterial cell could impact the protein levels in the secreted fraction independently of secretion, affecting our proposed model. Pairs of ESX-1 substrates require each other for stability (16, 32, 67, 80), and this is reflected as a loss of secretion in our study. For example, EsxB is not produced or secreted from the Δ*esxA* strain, and vice versa (Fig. 1*D*) (16, 67, 80)). Substrates regulate the expression of other substrates (21, 22). EspE and EspF negatively regulate *esxBA* expression (21). Although EsxA and EsxB accumulate in the Δ*espE* or Δ*espF* strains (ref. 21, and lane 8 in Fig. 1*D*), we did not measure a corresponding increase in EsxA/EsxB secretion. Finally, some substrates require each other for secretion but not production. For example, EspE is produced in but not secreted from the Δ*espF* strain (21). Because transcriptional and posttranscriptional regulation may impact ESX-1 substrate levels in the mycobacterial cell, transcriptome, proteome, and protein stability studies performed concurrently in this strain collection would be the best means to understand the dynamics of ESX-1 substrates in the mycobacterial cell and how this contributes to secretion.

Together, our comprehensive proteo-genetic analysis of ESX-1 secretion in *M. marinum* has provided a clear and testable model for the order of substrate secretion and for discrete roles of ESX-1 substrates in protein secretion. Using both approaches, we were able to define the degree of dependency of ESX-1 substrate secretion, contributing to our understanding of how ESX-1 substrates promote protein secretion.

Materials and Methods

M. marinum strains were generated from the M strain (WT; ATCC, BAA-525) (81, 82) and maintained as described (20, 21, 27). Strains and plasmids are listed in *SI Appendix*, Table S1. All oligonucleotide primers are listed in *SI Appendix*, Table S2. Hemolysis assays were performed as described (42, 68). RAW 264.7 cells (ATCC, TIB-71) were cultured and passaged as described (27). RAW cells were seeded at 2×10^5 cells/mL and infected at a multiplicity of infection of 5 (Fig. 1*C*; 1×10^6 cells/mL) and also infected at a multiplicity of infection of 2.5 (*SI Appendix*, Fig. S10; 5×10^5 cells/mL). Infections proceed for 2 h before gentamycin was added. Cytotoxicity assays and cell counts were performed as described (20, 21). Protein-secretion assays were performed as described (20, 21, 27). Secreted protein samples were prepared for mass-spectrometry proteomics as described in refs. 83 and 84). Protein digests were labeled with one vial of 8-plex iTRAQ reagent according to manufacturer's instructions. Individual sets of iTRAQ-labeled samples were subjected to nano-ultra-high performance liquid-chromatography–tandem mass spectrometry (nUHPLC-MS/MS) as in refs. 84 and 85. Triplicate mass spectrometry were acquired on a Q-Exactive HF instrument running an iTRAQ-adjusted TOP 15 acquisition. RAW files were converted to .mgf using MS-convert and protein-spectral matching, and iTRAQ quantification was performed using Protein Pilot with the Paragon Algorithm (54, 86) and background quantitative correction. RAW and converted files are available at Mass Spectrometry Interactive Virtual Environment (MassIVE): https://massive.ucsd.edu/ProteoSAFe/dataset.jsp?task=3ef07e4e883e40d782c7ee41af293e83 (MSV000088597) (PDX030584). Graphs for proteomic analyses were generated using R Studio. Replicates and the statistical analyses are in the figure legends. A detailed explanation of study methods is provided in the *SI Appendix*.

Data Availability. RAW and .mgf converted files have been publicly deposited in Mass Spectrometry Interactive Virtual Environment (MassIVE; https://massive.ucsd.edu/ProteoSAFe/static/massive.jsp) (MSV000088597/PDX030584).

ACKNOWLEDGMENTS. We thank Dr. Alexandra Chirakos for construction of the Δ*espC* strain, and Rebecca Prest for the models in *SI Appendix*, Fig. S6. We thank Dr. Bill Boggess in the Mass Spectrometry and Proteomics Core Facility at the University of Notre Dame. We thank the P.A.C. laboratory and Dr. Todd Gray (Department of Health, Wadsworth Center) for feedback. We thank Dr. Siyuan Zhang and Xiyu Liu (University of Notre Dame) for assistance in generating R code for the heat maps. Research reported in this publication was supported by the National Institute of Allergy and Infectious Diseases of the NIH under Award Number R21AI142127. The content is solely the responsibility of the authors and does not necessarily represent the official views of the NIH.

Author affiliations: [a]Department of Biological Sciences, University of Notre Dame, Notre Dame, IN 46556; and [b]Department of Chemistry and Biochemistry, University of Notre Dame, Notre Dame, IN 46556

1. R. Koch, [Tuberculosis etiology]. *Dtsch. Gesundheitsw.* **7**, 457–465 (1952).
2. V. Dartois, C. Sizemore, T. Dick, Editorial: NTM-the new uber-bugs. *Front. Microbiol.* **10**, 1299 (2019).
3. C. N. Ratnatunga *et al.*, The rise of non-tuberculosis mycobacterial lung disease. *Front. Immunol.* **11**, 303 (2020).
4. M. D. Johansen, J. L. Herrmann, L. Kremer, Non-tuberculous mycobacteria and the rise of *Mycobacterium abscessus*. *Nat. Rev. Microbiol.* **18**, 392–407 (2020).
5. F. Linell, A. Norden, *Mycobacterium balnei*, a new acid-fast bacillus occurring in swimming pools and capable of producing skin lesions in humans. *Acta Tuberc. Scand., Suppl.* **33**, 1–84 (1954).
6. D. M. Tobin, L. Ramakrishnan, Comparative pathogenesis of *Mycobacterium marinum* and *Mycobacterium tuberculosis*. *Cell. Microbiol.* **10**, 1027–1039 (2008).
7. J. A. Armstrong, P. D. Hart, Phagosome-lysosome interactions in cultured macrophages infected with virulent tubercle bacilli. Reversal of the usual nonfusion pattern and observations on bacterial survival. *J. Exp. Med.* **142**, 1–16 (1975).
8. J. A. Armstrong, P. D. Hart, Response of cultured macrophages to *Mycobacterium tuberculosis*, with observations on fusion of lysosomes with phagosomes. *J. Exp. Med.* **134**, 713–740 (1971).
9. R. Simeone *et al.*, Phagosomal rupture by *Mycobacterium tuberculosis* results in toxicity and host cell death. *PLoS Pathog.* **8**, e1002507 (2012).
10. N. van der Wel *et al.*, *M. tuberculosis* and *M. leprae* translocate from the phagolysosome to the cytosol in myeloid cells. *Cell* **129**, 1287–1298 (2007).
11. R. O. Watson, P. S. Manzanillo, J. S. Cox, Extracellular *M. tuberculosis* DNA targets bacteria for autophagy by activating the host DNA-sensing pathway. *Cell* **150**, 803–815 (2012).
12. Y. Cheng, J. S. Schorey, *Mycobacterium tuberculosis*-induced IFN-β production requires cytosolic DNA and RNA sensing pathways. *J. Exp. Med.* **215**, 2919–2935 (2018).
13. P. S. Manzanillo, M. U. Shiloh, D. A. Portnoy, J. S. Cox, *Mycobacterium tuberculosis* activates the DNA-dependent cytosolic surveillance pathway within macrophages. *Cell Host Microbe* **11**, 469–480 (2012).
14. D. Houben *et al.*, ESX-1-mediated translocation to the cytosol controls virulence of mycobacteria. *Cell. Microbiol.* **14**, 1287–1298 (2012).
15. T. Hsu *et al.*, The primary mechanism of attenuation of bacillus Calmette-Guérin is a loss of secreted lytic function required for invasion of lung interstitial tissue. *Proc. Natl. Acad. Sci. U.S.A.* **100**, 12420–12425 (2003).
16. S. A. Stanley, S. Raghavan, W. W. Hwang, J. S. Cox, Acute infection and macrophage subversion by *Mycobacterium tuberculosis* require a specialized secretion system. *Proc. Natl. Acad. Sci. U.S.A.* **100**, 13001–13006 (2003).
17. K. M. Guinn *et al.*, Individual RD1-region genes are required for export of ESAT-6/CFP-10 and for virulence of *Mycobacterium tuberculosis*. *Mol. Microbiol.* **51**, 359–370 (2004).
18. W. H. Conrad *et al.*, Mycobacterial ESX-1 secretion system mediates host cell lysis through bacterium contact-dependent gross membrane disruptions. *Proc. Natl. Acad. Sci. U.S.A.* **114**, 1371–1376 (2017).
19. B. McLaughlin *et al.*, A mycobacterium ESX-1-secreted virulence factor with unique requirements for export. *PLoS Pathog.* **3**, e105 (2007).
20. K. G. Sanchez *et al.*, EspM is a conserved transcription factor that regulates gene expression in response to the ESX-1 system. *MBio* **11**, e02807-19 (2020).

21. A. E. Chirakos, K. R. Nicholson, A. Huffman, P. A. Champion, Conserved ESX-1 substrates EspE and EspF are virulence factors that regulate gene expression. *Infect. Immun.* **88**, e00289-20 (2020).
22. A. E. Chirakos, A. Balaram, W. Conrad, P. A. Champion, Modeling tubercular ESX-1 secretion using *Mycobacterium marinum*. *Microbiol. Mol. Biol. Rev.* **84**, e00082-19 (2020).
23. E. N. Houben *et al.*, Composition of the type VII secretion system membrane complex. *Mol. Microbiol.* **86**, 472–484 (2012).
24. V. J. van Winden *et al.*, Mycosins are required for the stabilization of the ESX-1 and ESX-5 type VII secretion membrane complexes. *MBio* **7**, e01471-16 (2016).
25. K. S. Beckham *et al.*, Structure of the mycobacterial ESX-5 type VII secretion system membrane complex by single-particle analysis. *Nat. Microbiol.* **2**, 17047 (2017).
26. R. E. Bosserman, P. A. Champion, Esx systems and the mycobacterial cell envelope: What's the connection? *J. Bacteriol.* **199**, e00131-17 (2017).
27. R. E. Bosserman, K. R. Nicholson, M. M. Champion, P. A. Champion, A new ESX-1 substrate in *Mycobacterium marinum* that is required for hemolysis but not host cell lysis. *J. Bacteriol.* **201**, e00760-18 (2019).
28. R. E. Bosserman, C. R. Thompson, K. R. Nicholson, P. A. Champion, Esx paralogs are functionally equivalent to ESX-1 proteins but are dispensable for virulence in *Mycobacterium marinum*. *J. Bacteriol.* **200**, e00726-17 (2018).
29. U. Tak, T. Dokland, M. Niederweis, Pore-forming Esx proteins mediate toxin secretion by *Mycobacterium tuberculosis*. *Nat. Commun.* **12**, 394 (2021).
30. Q. Wang *et al.*, PE/PPE proteins mediate nutrient transport across the outer membrane of *Mycobacterium tuberculosis*. *Science* **367**, 1147–1151 (2020).
31. S. J. Dechow, J. J. Baker, M. R. Murto, R. B. Abramovitch, *ppe51* variants promote non-replicating *Mycobacterium tuberculosis* to grow at acidic pH by selectively promoting glycerol uptake. *bioRxiv* Preprint (19 May 2021). 10.1101/2021.05.19.444820.
32. Y. Lou, J. Rybniker, C. Sala, S. T. Cole, EspC forms a filamentous structure in the cell envelope of *Mycobacterium tuberculosis* and impacts ESX-1 secretion. *Mol. Microbiol.* **103**, 26–38 (2017).
33. J. Piton, F. Pojer, S. Wakatsuki, C. Gati, S. T. Cole, High resolution CryoEM structure of the ring-shaped virulence factor EspB from *Mycobacterium tuberculosis*. *J. Struct. Biol.* **4**, 100029 (2020).
34. M. Solomonson *et al.*, Structure of EspB from the ESX-1 type VII secretion system and insights into its export mechanism. *Structure* **23**, 571–583 (2015).
35. J. Lienard *et al.*, The *Mycobacterium marinum* ESX-1 system mediates phagosomal permeabilization and type I interferon production via separable mechanisms. *Proc. Natl. Acad. Sci. U.S.A.* **117**, 1160–1166 (2020).
36. Q. Guo, J. Bi, H. Wang, X. Zhang, *Mycobacterium tuberculosis* ESX-1-secreted substrate protein EspC promotes mycobacterial survival through endoplasmic reticulum stress-mediated apoptosis. *Emerg. Microbes Infect.* **10**, 19–36 (2021).
37. S. M. Fortune *et al.*, Mutually dependent secretion of proteins required for mycobacterial virulence. *Proc. Natl. Acad. Sci. U.S.A.* **102**, 10676–10681 (2005).
38. P. A. Champion, M. M. Champion, P. Manzanillo, J. S. Cox, ESX-1 secreted virulence factors are recognized by multiple cytosolic AAA ATPases in pathogenic mycobacteria. *Mol. Microbiol.* **73**, 950–962 (2009).
39. M. M. Champion, E. A. Williams, R. S. Pinapati, P. A. Champion, Correlation of phenotypic profiles using targeted proteomics identifies mycobacterial esx-1 substrates. *J. Proteome Res.* **13**, 5151–5164 (2014).
40. F. Carlsson, S. A. Joshi, L. Rangell, E. J. Brown, Polar localization of virulence-related Esx-1 secretion in mycobacteria. *PLoS Pathog.* **5**, e1000285 (2009).
41. A. Kapopoulou, J. M. Lew, S. T. Cole, The MycoBrowser portal: A comprehensive and manually annotated resource for mycobacterial genomes. *Tuberculosis (Edinb.)* **91**, 8–13 (2011).
42. L. Y. Gao *et al.*, A mycobacterial virulence gene cluster extending RD1 is required for cytolysis, bacterial spreading and ESAT-6 secretion. *Mol. Microbiol.* **53**, 1677–1693 (2004).
43. J. M. Chen *et al.*, *Mycobacterium tuberculosis* EspB binds phospholipids and mediates EsxA-independent virulence. *Mol. Microbiol.* **89**, 1154–1166 (2013).
44. J. M. Chen *et al.*, Phenotypic profiling of *Mycobacterium tuberculosis* EspA point mutants reveals that blockage of ESAT-6 and CFP-10 secretion in vitro does not always correlate with attenuation of virulence. *J. Bacteriol.* **195**, 5421–5430 (2013).
45. J. M. Chen *et al.*, EspD is critical for the virulence-mediating ESX-1 secretion system in *Mycobacterium tuberculosis*. *J. Bacteriol.* **194**, 884–893 (2012).
46. P. A. Champion, Disconnecting in vitro ESX-1 secretion from mycobacterial virulence. *J. Bacteriol.* **195**, 5418–5420 (2013).
47. R. Wassermann *et al.*, *Mycobacterium tuberculosis* differentially activates cGAS- and inflammasome-dependent intracellular immune responses through ESX-1. *Cell Host Microbe* **17**, 799–810 (2015).
48. K. R. Nicholson, C. B. Mousseau, M. M. Champion, P. A. Champion, The genetic proteome: Using genetics to inform the proteome of mycobacterial pathogens. *PLoS Pathog.* **17**, e1009124 (2021).
49. K. M. George, Y. Yuan, D. R. Sherman, C. E. Barry, 3rd, The biosynthesis of cyclopropanated mycolic acids in *Mycobacterium tuberculosis*. Identification and functional analysis of CMAS-2. *J. Biol. Chem.* **270**, 27292–27298 (1995).
50. F. Mba Medie, M. M. Champion, E. A. Williams, P. A. D. Champion, Homeostasis of N-α-terminal acetylation of EsxA correlates with virulence in *Mycobacterium marinum*. *Infect. Immun.* **82**, 4572–4586 (2014).
51. M. M. Osman, A. J. Pagán, J. K. Shanahan, L. Ramakrishnan, *Mycobacterium marinum* phthiocerol dimycocerosates enhance macrophage phagosomal permeabilization and membrane damage. *PLoS One* **15**, e0233252 (2020).
52. P. S. Renshaw *et al.*, Sequence-specific assignment and secondary structure determination of the 195-residue complex formed by the *Mycobacterium tuberculosis* proteins CFP-10 and ESAT-6. *J. Biomol. NMR* **30**, 225–226 (2004).
53. R. E. Bosserman *et al.*, WhiB6 regulation of ESX-1 gene expression is controlled by a negative feedback loop in *Mycobacterium marinum*. *Proc. Natl. Acad. Sci. U.S.A.* **114**, E10772–E10781 (2017).
54. I. V. Shilov *et al.*, The Paragon Algorithm, a next generation search engine that uses sequence temperature values and feature probabilities to identify peptides from tandem mass spectra. *Mol. Cell. Proteomics* **6**, 1638–1655 (2007).
55. H. Målen, F. S. Berven, K. E. Fladmark, H. G. Wiker, Comprehensive analysis of exported proteins from *Mycobacterium tuberculosis* H37Rv. *Proteomics* **7**, 1702–1718 (2007).
56. G. A. de Souza, N. A. Leversen, H. Målen, H. G. Wiker, Bacterial proteins with cleaved or uncleaved signal peptides of the general secretory pathway. *J. Proteomics* **75**, 502–510 (2011).
57. S. Gu *et al.*, Comprehensive proteomic profiling of the membrane constituents of a *Mycobacterium tuberculosis* strain. *Mol. Cell. Proteomics* **2**, 1284–1296 (2003).
58. L. M. Wolfe, S. B. Mahaffey, N. A. Kruh, K. M. Dobos, Proteomic definition of the cell wall of *Mycobacterium tuberculosis*. *J. Proteome Res.* **9**, 5816–5826 (2010).
59. J. Mattow *et al.*, Comparative proteome analysis of culture supernatant proteins from virulent *Mycobacterium tuberculosis* H37Rv and attenuated *M. bovis* BCG Copenhagen. *Electrophoresis* **24**, 3405–3420 (2003).
60. J. G. Canestrari *et al.*, Polycysteine-encoding leaderless short ORFs function as cysteine-responsive attenuators of operonic gene expression in mycobacteria. *Mol. Microbiol.* **114**, 93–108 (2020).
61. J. J. Almagro Armenteros *et al.*, SignalP 5.0 improves signal peptide predictions using deep neural networks. *Nat. Biotechnol.* **37**, 420–423 (2019).
62. W. Deng *et al.*, Assembly, structure, function and regulation of type III secretion systems. *Nat. Rev. Microbiol.* **15**, 323–337 (2017).
63. L. M. Okkels *et al.*, PPE protein (Rv3873) from DNA segment RD1 of *Mycobacterium tuberculosis*: Strong recognition of both specific T-cell epitopes and epitopes conserved within the PPE family. *Infect. Immun.* **71**, 6116–6123 (2003).
64. D. Pajuelo *et al.*, Toxin secretion and trafficking by *Mycobacterium tuberculosis*. *Nat. Commun.* **12**, 6592 (2021).
65. L. S. Ates *et al.*, Essential role of the ESX-5 secretion system in outer membrane permeability of pathogenic mycobacteria. *PLoS Genet.* **11**, e1005190 (2015).
66. A. Rivera-Calzada, N. Famelis, O. Llorca, S. Geibel, Type VII secretion systems: Structure, functions and transport models. *Nat. Rev. Microbiol.* **19**, 567–584 (2021).
67. K. L. Lightbody *et al.*, Characterisation of complex formation between members of the *Mycobacterium tuberculosis* complex CFP-10/ESAT-6 protein family: Towards an understanding of the rules governing complex formation and thereby functional flexibility. *FEMS Microbiol. Lett.* **238**, 255–262 (2004).
68. M. M. Champion, E. A. Williams, G. M. Kennedy, P. A. Champion, Direct detection of bacterial protein secretion using whole colony proteomics. *Mol. Cell. Proteomics* **11**, 596–604 (2012).
69. B. Callahan *et al.*, Conservation of structure and protein-protein interactions mediated by the secreted mycobacterial proteins EsxA, EsxB, and EspA. *J. Bacteriol.* **192**, 326–335 (2010).
70. Y. M. Ohol *et al.*, *Mycobacterium tuberculosis* MycP1 protease plays a dual role in regulation of ESX-1 secretion and virulence. *Cell Host Microbe* **7**, 210–220 (2010).
71. Z. L. Lim, K. Drever, N. Dhar, S. T. Cole, J. M. Chen, *Mycobacterium tuberculosis* EspK has active but distinct roles in the secretion of EsxA and EspB. *J. Bacteriol.* **204**, e0006022 (2022).
72. M. R. Diaz, J. M. King, T. L. Yahr, Intrinsic and extrinsic regulation of Type III secretion gene expression in *Pseudomonas aeruginosa*. *Front. Microbiol.* **2**, 89 (2011).
73. M. L. McCaw, G. L. Lykken, P. K. Singh, T. L. Yahr, ExsD is a negative regulator of the *Pseudomonas aeruginosa* type III secretion regulon. *Mol. Microbiol.* **46**, 1123–1133 (2002).
74. A. Nadeem *et al.*, A tripartite cytolytic toxin formed by *Vibrio cholerae* proteins with flagellum-facilitated secretion. *Proc. Natl. Acad. Sci. U.S.A.* **118**, e2111418118 (2021).
75. J. A. MacGurn, S. Raghavan, S. A. Stanley, J. S. Cox, A non-RD1 gene cluster is required for Snm secretion in *Mycobacterium tuberculosis*. *Mol. Microbiol.* **57**, 1653–1663 (2005).
76. J. A. MacGurn, J. S. Cox, A genetic screen for *Mycobacterium tuberculosis* mutants defective for phagosome maturation arrest identifies components of the ESX-1 secretion system. *Infect. Immun.* **75**, 2668–2678 (2007).
77. H. Sato, M. L. Hunt, J. J. Weiner, A. T. Hansen, D. W. Frank, Modified needle-tip PcrV proteins reveal distinct phenotypes relevant to the control of type III secretion and intoxication by *Pseudomonas aeruginosa*. *PLoS One* **6**, e18356 (2011).
78. L. Journet, C. Agrain, P. Broz, G. R. Cornelis, The needle length of bacterial injectisomes is determined by a molecular ruler. *Science* **302**, 1757–1760 (2003).
79. C. Sala *et al.*, EspL is essential for virulence and stabilizes EspE, EspF and EspH levels in *Mycobacterium tuberculosis*. *PLoS Pathog.* **14**, e1007491 (2018).
80. P. S. Renshaw *et al.*, Structure and function of the complex formed by the tuberculosis virulence factors CFP-10 and ESAT-6. *EMBO J.* **24**, 2491–2498 (2005).
81. E. A. Williams *et al.*, A nonsense mutation in *Mycobacterium marinum* that is suppressible by a novel mechanism. *Infect. Immun.* **85**, e00653-16 (2017).
82. T. Parish, N. G. Stoker, Use of a flexible cassette method to generate a double unmarked *Mycobacterium tuberculosis* tlyA plcABC mutant by gene replacement. *Microbiology (Reading)* **146**, 1969–1975 (2000).
83. P. A. Champion, S. A. Stanley, M. M. Champion, E. J. Brown, J. S. Cox, C-terminal signal sequence promotes virulence factor secretion in *Mycobacterium tuberculosis*. *Science* **313**, 1632–1636 (2006).
84. L. Sun *et al.*, Quantitative proteomics of *Xenopus laevis* embryos: Expression kinetics of nearly 4000 proteins during early development. *Sci. Rep.* **4**, 4365 (2014).
85. E. H. Peuchen *et al.*, Phosphorylation dynamics dominate the regulated proteome during early *Xenopus* development. *Sci. Rep.* **7**, 15647 (2017).
86. W. H. Tang, I. V. Shilov, S. L. Seymour, Nonlinear fitting method for determining local false discovery rates from decoy database searches. *J. Proteome Res.* **7**, 3661–3667 (2008).